OBSERVATIONS OF FAR-ULTRAVIOLET DIFFUSE EMISSION FROM THE SMALL MAGELLANIC CLOUD

Ananta C. Pradhan, Jayant Murthy, and Amit Pathak[1]
Indian Institute of Astrophysics, Bangalore 560 034, India; acp@iiap.res.in

ABSTRACT

We report the first observations of far-ultraviolet (FUV: 1000–1150 Å) diffuse radiation from the Small Magellanic Cloud (SMC) using observations from the *Far-Ultraviolet Spectroscopic Explorer*. The strength of FUV diffuse surface brightness in the SMC ranges from the detection limit of 2000 photons cm^{-2} s^{-1} sr^{-1} $Å^{-1}$ to a maximum of 3×10^5 photons cm^{-2} s^{-1} sr^{-1} $Å^{-1}$ at 1004 Å. The contribution of diffuse emission to the total radiation field was found to be 34% at 1004 Å to 44% at 1117 Å with a maximum observed uncertainty of 30%. There is a striking difference between the FUV diffuse fraction from the SMC and the Large Magellanic Cloud with the SMC fraction being higher probably because of the higher dust albedo. The FUV diffuse emission correlates with Hα emission in the H II regions of the SMC.

Key words: Magellanic Clouds – ultraviolet: ISM

1. INTRODUCTION

The Small Magellanic Cloud (SMC) is a nearby dwarf galaxy (≈60 kpc; Hilditch et al. 2005) which provides an ideal environment to study the interstellar medium (ISM) in a region of low metallicity ($Z \approx 0.005$; Dufour 1984; Asplund et al. 2004). The foreground Galactic extinction is low ($E(B-V) = 0.02$ mag; Hutchings 1982) and its face-on view orientation allows the observer to investigate the small-scale structures. The SMC itself contains significant amounts of dust and gas but with a low dust-to-gas ratio (8 times smaller than the Milky Way; Bouchet et al. 1985), and a strong interstellar ultraviolet (UV) radiation field (4–10 times higher than that in the solar neighborhood; Vangioni-Flam et al. 1980). The ISM of the SMC is similar to that of high-redshift galaxies because of its low metallicity and therefore may be a stepping stone to our understanding of the ISM within them (Witt & Gordon 2000). Dust in the SMC is quite different from that in either the Milky Way or the Large Magellanic Cloud (LMC) as shown, for instance, by the absence of the 2175 Å bump (Gordon et al. 2003). Models of the dust in the SMC typically assume that it is dominated by silicates with the absence of the 2175 Å bump attributed to a lack of carbonaceous dust (Weingartner & Draine 2001).

The surface brightness and integrated magnitudes of the bright regions of the SMC have been mapped in the near-ultraviolet (NUV) by a number of rocket and satellite observations (Nandy et al. 1978; Vangioni-Flam et al. 1980; Maucherat-Joubert et al. 1980; Cornett et al. 1994). Here, we present the first observations of diffuse far-UV (FUV: 1000–1150 Å) emission from the SMC. These were serendipitous observations made with the *Far-Ultraviolet Spectroscopic Explorer* (*FUSE*) and include different environments in the SMC: from those near hot stars to those further out at the edges of the galaxy. The diffuse emission tracks the interaction of the radiation field with the dust and is an important input into models of distant galaxies (da Cunha et al. 2008). The SMC offers an opportunity to test these models at high spatial resolution and to distinguish the different components of the galaxy.

2. OBSERVATIONS AND DATA ANALYSIS

We have used observations made by the *FUSE* spacecraft to measure the diffuse emission from the SMC in the FUV. The *FUSE* instrument and its mission have been discussed by Moos et al. (2000) and Sahnow et al. (2000). It consisted of four optical channels with each channel comprising a mirror, focal plane assembly (FPA), and diffraction grating. Two of the channels included optics coated with LiF and aluminum and the other two with SiC, and each channel was imaged onto a delay-line detector at the focal plane. Observations were made through three different apertures: the high-resolution aperture (HIRS: $1''.25 \times 20''$), the medium-resolution aperture (MDRS: $4'' \times 20''$), and the low-resolution aperture (LWRS: $30'' \times 30''$), with all three obtaining data simultaneously. Thus, even though a source may have been observed in the MDRS or HIRS aperture, the diffuse background could still be measured through the LWRS aperture as it is separated from the former apertures by $100''$ and $200''$, respectively. Only the very brightest backgrounds could be observed with the smaller MDRS aperture or with the less sensitive SiC channels. Murthy & Sahnow (2004) have shown that the practical limit for *FUSE* diffuse observation is about 2000 photons cm^{-2} s^{-1} sr^{-1} $Å^{-1}$.

There were a total of 220 *FUSE* observations within $5°$ of the SMC but 190 were of stars through the LWRS aperture leaving 30 pointings from which we could extract the diffuse background. These observations were from two classes of targets: stars observed through either of the MDRS or HIRS apertures, or empty areas of the sky where the spectrographs were allowed to thermalize before an instrumental realignment. The observational details of these targets are given in Table 1. Most of the regions observed are either active areas of star formation or H II regions, such as NGC 346 and NGC 330.

The data selection and analysis procedure have been explained in detail elsewhere (Murthy & Sahnow 2004). We began with the raw photon list and processed the data through the latest version of CalFUSE (v3.2; Dixon et al. 2007) except that we estimated the instrumental background from the counts in the detector just off the spectrum. The background was subtracted from the data which was then collapsed into two wavelength bands per segment, avoiding airglow lines. This resulted in a total of six bands from three segments. We

---

Table 1
Details of the *FUSE* Diffuse Observations in the SMC

FUSE ID	R.A.[a]	Decl.[a]	LiF 1A1[b]	LiF 1A2[b]	LiF 1B1[b]	LiF 1B2[b]	*UIT*[c]
G9310201	00 46 38	−73 08 24	1.33 ± 0.83	1.43 ± 0.36	1.56 ± 0.45	2.26 ± 0.53	16.02
G9310301	00 47 16	−73 08 24	0.97 ± 0.40	2.15 ± 0.22	2.56 ± 0.34	3.11 ± 0.38	32.96
G9310401	00 48 26	−73 19 12	2.78 ± 0.68	4.99 ± 0.29	6.62 ± 0.53	7.13 ± 0.65	24.69
G9310501	00 49 02	−73 14 24	3.28 ± 0.24	4.90 ± 0.13	5.78 ± 0.27	5.78 ± 0.24	18.90
G9310601	00 51 07	−73 21 36	9.07 ± 0.22	11.33 ± 0.11	11.09 ± 0.26	10.40 ± 0.28	13.57
F3230101	00 53 07	−74 39 00	3.87 ± 0.39	0.75 ± 0.63	0.48 ± 0.40	0.32 ± 0.29	4.19
F3230102	00 53 07	−74 39 00	0.15 ± 0.15	0.10 ± 0.09	0.28 ± 0.20	0.29 ± 0.23	7.84
F3230103	00 53 07	−74 39 00	0.87 ± 0.57	1.22 ± 0.40	0.94 ± 0.15	1.24 ± 0.15	11.25
F3230104	00 53 07	−74 39 00	0.12 ± 0.12	0.16 ± 0.11	0.27 ± 0.23	0.25 ± 0.14	7.61
F3230105	00 53 07	−74 39 00	0.15 ± 0.15	0.46 ± 0.32	0.40 ± 0.27	0.51 ± 0.27	
F3230106	00 53 07	−74 39 00	0.25 ± 0.15	0.78 ± 0.06	0.64 ± 0.34	0.76 ± 0.23	
D9110901	00 53 57	−70 37 48	0.22 ± 0.19	0.46 ± 0.41	0.22 ± 0.19	0.46 ± 0.41	
G9310701	00 58 19	−72 17 24	10.07 ± 0.17	12.81 ± 0.10	13.69 ± 0.23	12.45 ± 0.22	
P2030201	00 59 36	−72 07 48	17.03 ± 0.24	20.47 ± 0.17	25.15 ± 0.35	23.28 ± 0.36	
C1580101	00 59 43	−72 09 36	3.50 ± 0.25	4.80 ± 0.13	5.72 ± 0.24	5.81 ± 0.30	
S4057101	01 00 09	−72 08 24	8.96 ± 0.13	10.69 ± 0.07	9.63 ± 0.21	9.46 ± 0.18	
G9310801	01 00 24	−71 33 36	5.78 ± 0.24	7.76 ± 0.16	9.35 ± 0.27	7.98 ± 0.34	
G9310901	01 03 16	−72 09 36	15.90 ± 0.23	20.27 ± 0.12	22.02 ± 0.24	19.86 ± 0.22	
G9311002	01 03 33	−72 02 24	20.30 ± 0.27	24.25 ± 0.14	25.15 ± 0.22	23.29 ± 0.28	
C0830201	01 03 36	−71 58 48	14.64 ± 0.39	18.29 ± 0.17	16.64 ± 0.41	18.24 ± 0.41	
G0350101	01 03 48	−71 58 12	5.31 ± 0.22	6.79 ± 0.12	7.67 ± 0.21	7.48 ± 0.25	
E5110802	01 03 52	−72 54 00	2.69 ± 0.46	3.77 ± 0.20	4.41 ± 0.40	4.57 ± 0.44	
F3210103	01 03 52	−72 07 48	17.09 ± 0.12	24.79 ± 0.07	34.14 ± 0.15	33.34 ± 0.14	
F3210104	01 03 52	−72 07 48	22.18 ± 0.25	33.53 ± 0.11	46.05 ± 0.17	45.32 ± 0.21	
E5110801	01 03 57	−72 54 36	0.70 ± 0.52	0.86 ± 0.45	0.92 ± 0.40	0.90 ± 0.50	
A0750204	01 04 00	−72 01 48	24.65 ± 0.30	34.22 ± 0.16	30.03 ± 0.28	28.92 ± 0.27	
C0830302	01 04 33	−71 59 24	2.97 ± 0.24	3.31 ± 0.17	2.92 ± 0.18	2.78 ± 0.19	
G0350301	01 04 48	−72 01 12	8.17 ± 0.31	10.21 ± 0.17	9.93 ± 0.26	9.34 ± 0.40	
D9044301	01 05 12	−72 23 24	0.95 ± 0.17	1.32 ± 0.08	0.55 ± 0.09	0.71 ± 0.12	
D9044401	01 06 19	−72 05 24	1.85 ± 1.85	0.88 ± 0.27	1.64 ± 1.20	0.78 ± 0.57	

Notes.
[a] R.A. and decl. represent the *FUSE* LWRS position. Units of right ascension are hours, minutes, and seconds; units of declination are degrees, arcminutes, and arcseconds.
[b] The surface brightness of the diffuse radiation observed in the *FUSE* bands is in units of 10^4 photons cm^{-2} s^{-1} sr^{-1} Å^{-1} and the uncertainties are 1σ error bar.
[c] *UIT* surface brightness in units of 10^4 photons cm^{-2} s^{-1} sr^{-1} Å^{-1} and the error in the data is around 15% (Cornett et al. 1997).

found that the data were of much higher quality from segment 1, leaving us with four bands at effective wavelengths of 1004 Å (1A1), 1058 Å (1A2), 1117 Å (1B1), and 1157 Å (1B2).

The surface brightness measured in the *FUSE* bands shows a strong correlation between each of them with correlation coefficients of better than 0.9. Our observed surface brightnesses (Table 1) range from near the *FUSE* detection limit to as high as 3×10^5 photons cm^{-2} s^{-1} sr^{-1} Å^{-1} in NGC 346, the youngest and largest H II region in the SMC. We have estimated the level of Galactic background at these wavelengths from the *Voyager* maps of Murthy et al. (1999) to be about 1000 photons cm^{-2} s^{-1} sr^{-1} Å^{-1}, much less than the observed SMC fluxes.

3. RESULTS AND DISCUSSION

We have plotted the location of our targets (plus symbols) on a 160 μm image of the SMC (Gordon et al. 2009) in Figure 1. Also shown are the 40′ fields (circles) observed by *Ultraviolet Imaging Telescope* (*UIT*) at 1615 Å, covering most of the SMC Bar (Cornett et al. 1997). We calculated the diffuse NUV flux for the nine *FUSE* locations that are within the *UIT* field of observations by integrating the 1″.13 *UIT* pixels over the 30″ × 30″ *FUSE* LWRS aperture. These fluxes are listed in Table 1. The *UIT* fluxes are highly correlated with the surface
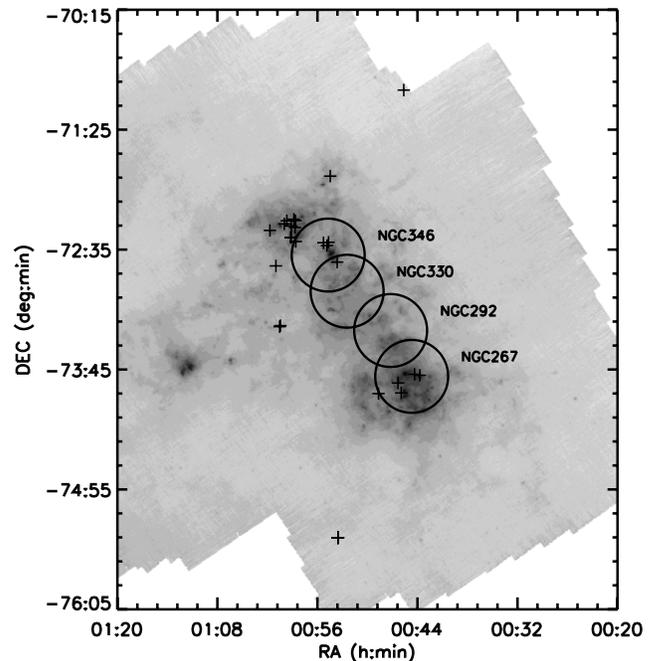
Figure 1. IR 160 μm image of the SMC from Gordon et al. (2009) showing the position of the diffuse *FUSE* targets marked by "+" symbols. 40′ diameter *UIT* observations are shown by circles.
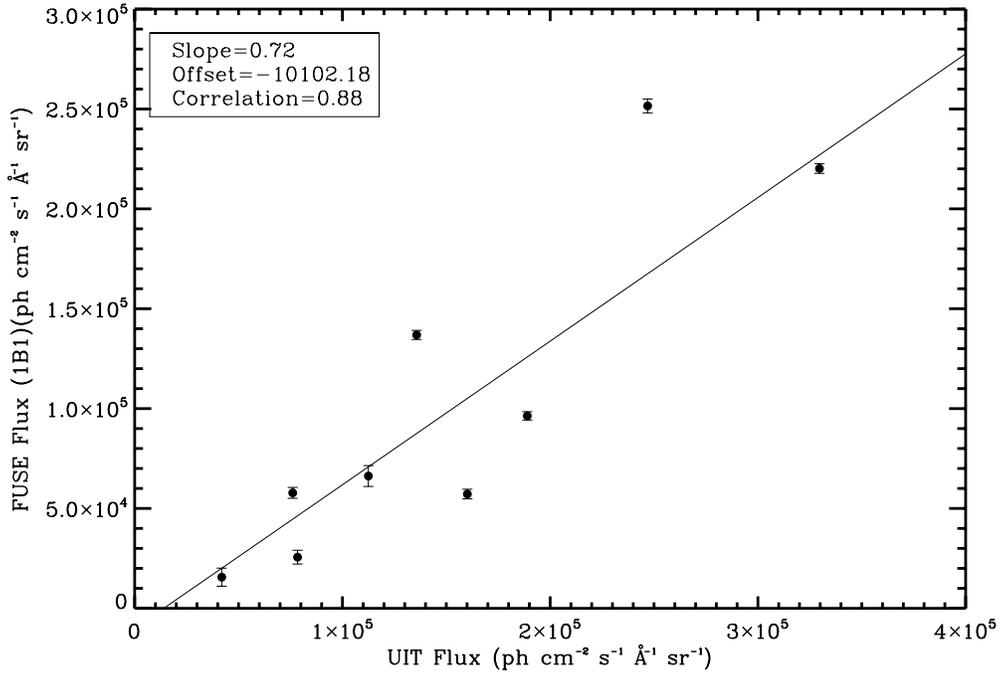
Figure 2. Correlation between the *FUSE* (1B1) and the *UIT* surface brightness is shown. The correlation coefficient is 0.88. The best-fit line has slope 0.72 and an offset of -10102.18 photons cm^{-2} s^{-1} sr^{-1} Å^{-1}. Errors in the *FUSE* observations are shown by vertical bars and the error in the *UIT* observations is 15%.
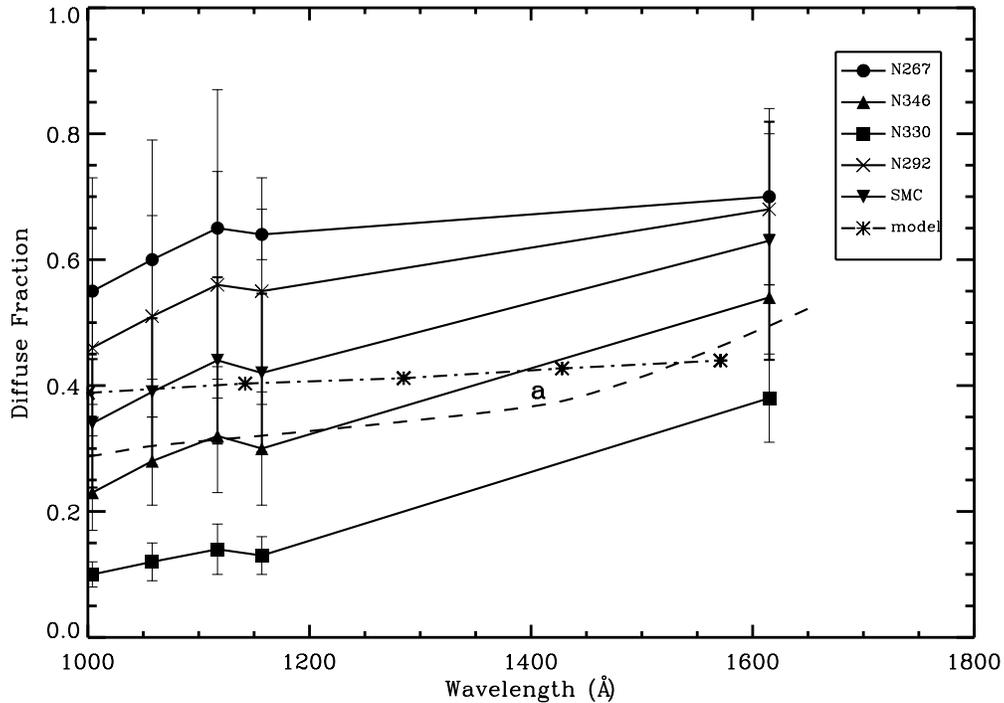
Figure 3. Variation of diffuse fraction against the wavelength for the *UIT* regions as well as for the SMC bar as a whole. The dust albedo (dashed line) is from the model calculations of Weingartner & Draine (2001). The error bars were empirically calculated by taking the extremes of the observed fluxes. The model calculation of diffuse fraction (dot-dashed line) is from Witt & Gordon (2000).

brightness of the *FUSE* bands with a correlation coefficient of better than 0.88 (Figure 2).

The fraction of the total (stellar + diffuse) FUV light emitted as diffuse radiation in the SMC provides important information in context to the regional distribution of dust. We found the total flux in each of the *UIT* fields by summing the fluxes in all pixels in that field. We then used the catalog of Cornett et al. (1997) to calculate the total stellar flux in each field. The diffuse

flux in the *UIT* field was the difference between the two. We extended the stellar flux into the *FUSE* bands using Kurucz (Kurucz 1992) model spectra and calculated their flux in *FUSE* bands. Finally, we extrapolated the diffuse flux into the *FUSE* bands using the observed *FUSE/UIT* diffuse flux ratios, i.e., the slope of the best-fit line (Figure 2), obtained separately for each of the *FUSE* bands from their correlation with the *UIT* band. Cornett et al. (1997) predicted that 22% of the diffuse
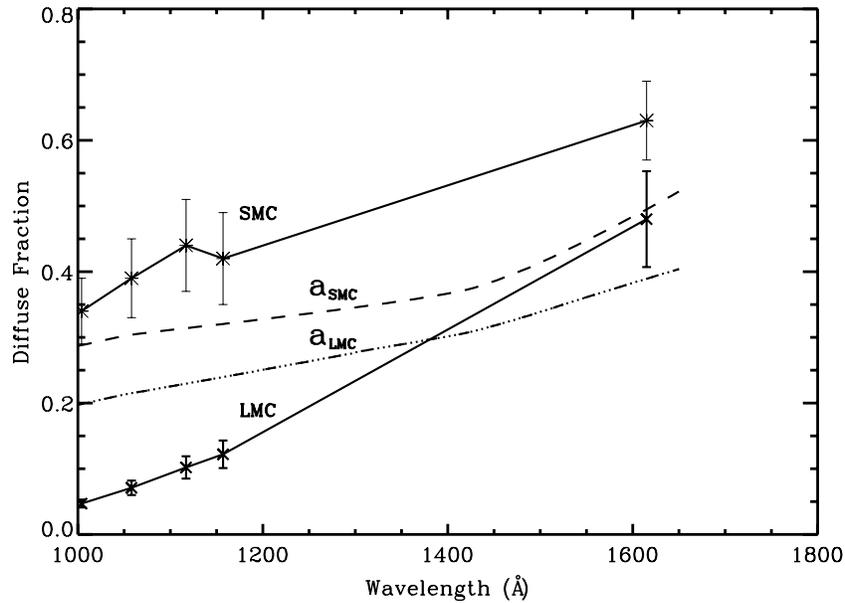
Figure 4. Comparison of diffuse FUV fraction of the LMC and the SMC. The dashed line represents the albedo of the SMC and the dot-dashed line represents the albedo of the LMC and are obtained from the model calculations of Weingartner & Draine (2001).
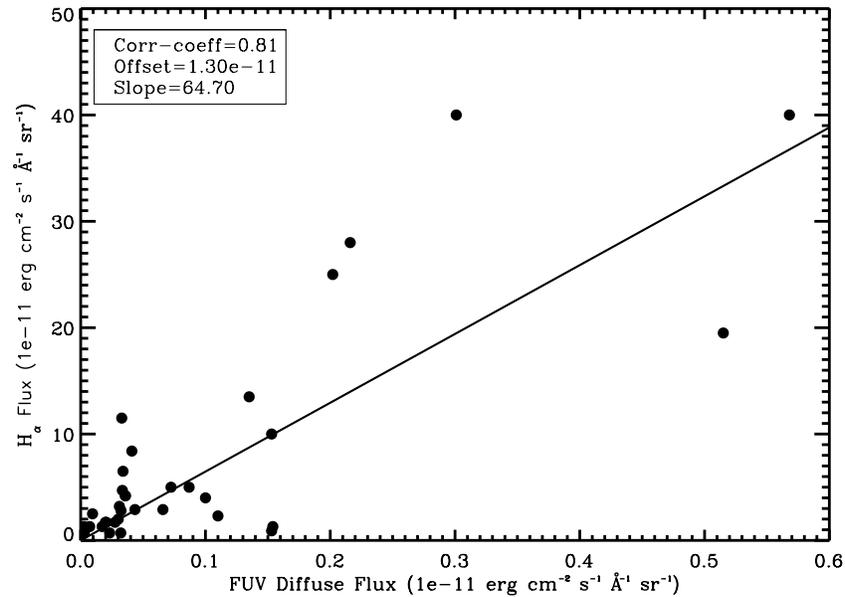
Figure 5. Plot of the FUV diffuse flux and the Hα flux of the H ɪɪ regions of the SMC (Kennicutt & Hodge 1986). The best-fit line has slope 64.70 and an offset of 1.30×10^{-11} erg cm^{-2} s^{-1} sr^{-1} Å^{-1}. The correlation coefficient is 0.81.

flux was due to faint unresolved stars which we subtracted from each of the *UIT* and *FUSE* diffuse fluxes. The diffuse fraction, defined as the diffuse emission divided by the total emission, was then calculated for each region and over the entire SMC Bar (Figure 3), with an estimated uncertainty of about 30%. In all cases, the behavior of the diffuse fraction is almost the same, rising by 10% from 1000 Å to 1150 Å and a further 50% from 1150 Å to 1615 Å. The albedo of the dust obtained from the theoretical predictions of Weingartner & Draine (2001) for a mix of spherical carbonaceous and silicate grains increases by about the same factor over the considered wavelength range and the consequent increase in scattered light may be responsible for the increased diffuse fraction at longer wavelengths.

Integrating over the entire SMC Bar, we find that 34% of the total radiation that escapes the SMC Bar at 1004 Å is diffuse,

rising to 63% at 1615 Å. The scattered light in the SMC has been modeled by Witt & Gordon (2000) using multiple scattering in a clumpy medium. They found that the diffuse radiation is 25%–50% of the total (Figure 3) depending on different dust geometries. Considering only H ɪɪ regions of the SMC, we found that around 20% of the total radiation at 1004 Å is diffuse, rising to 50% at 1615 Å. Studies for the Orion nebula (Bohlin et al. 1982) and NGC 595 (Malumuth et al. 1996) find similar results with 66% of the total radiation being diffuse at 1400 Å in Orion and 55% at 1700 Å in NGC 595. Pradhan et al. (2010) found significantly smaller values for the diffuse fraction in the LMC (Figure 4) perhaps due to the difference in grain size and composition between the two galaxies (Pei 1992; Weingartner & Draine 2001; Gordon et al. 2003). The albedo of the SMC dust is about 50% higher (Weingartner & Draine 2001) compared

to the LMC dust (Figure 4) and this may explain the increased diffuse fraction in the SMC.

We have examined the variation of the diffuse fraction over different regions in the SMC bar, and find that it is larger in those areas where there are fewer stars (NGC 267 and NGC 292), which suggests that much of the diffuse radiation from those regions is actually due to distant stars. Similar results were found for the LMC (Pradhan et al. 2010) which show that the diffuse fraction is less in crowded regions such as 30 Doradus, SN 1987A, and N11 (4%–10%) and more in sparse regions such as N70 (24%–45%). Cole et al. (1999) modeled the escape fraction of NUV photons for the LMC where they show that much of the stellar light is non-local, i.e., the light from the distant OB associations is scattered by local dust.

A catalog of H II regions in the SMC was given by Davies et al. (1976) and their integrated Hα flux was calculated by Kennicutt & Hodge (1986). We have computed the integrated FUV diffuse flux in the *FUSE* bands for 36 H II regions defined by Cornett et al. (1997). We find a good correlation ($r = 0.81$) between the integrated diffuse FUV emission and Hα emission from H II regions of the SMC (Figure 5). This is as expected given that the Hα flux is proportional to the brightness of the exciting stars as is FUV flux.

4. CONCLUSIONS

We have measured FUV diffuse emissions in the SMC using spectra obtained by *FUSE* from different environments. The diffuse radiation is primarily due to light from hot stars scattered by the interstellar dust grains. We have used these observations to measure the FUV diffuse fraction which is 34%–44% in the *FUSE* bands (1000–1150 Å), increasing up to 63% at 1615 Å. The amount of light scattered increases toward the longer wavelengths showing that a large percentage of the light at shorter wavelengths is absorbed by the dust.

The behavior and distribution of FUV diffuse emission and emission fraction are quite similar in both the LMC and the SMC with much of the stellar radiation in both galaxies being non-local, i.e., the diffuse (scattered) light in a particular region is the light coming from distant stars being scattered by local dust. The diffuse fraction in the SMC is higher than in the LMC and the difference in diffuse fraction is related to the amount of dust, dust grain properties, and geometry. A more detailed model incorporating the ample amount of data available for both galaxies in other spectral band is in progress to sort out the effect of local geometry from dust scattering. We found a good correlation between FUV diffuse emission and the Hα emission in the H II regions.

REFERENCES

Asplund, M., Grevesse, N., Sauval, A. J., Allende, P. C., & Kiselman, D. 2004, A&A, 417, 751
Bohlin, R. C., Hill, J. K., Stecher, T. P., & Witt, A. N. 1982, ApJ, 255, 87
Bouchet, P., Lequeux, J., Maurice, E., Prevot, L., & Prevot-Burnichon, M. L. 1985, A&A, 149, 330
Cole, A. A., Nordsieck, K. H., Gibson, S. J., & Harris, W. M. 1999, AJ, 118, 2292
Cornett, R. H., Greason, M. R., Hill, J. K., Parker, J. Wm., & Waller, W. H. 1997, AJ, 113, 1011
Cornett, R. H., Hill, J. K., Bohlin, R. C., et al. 1994, ApJ, 425, L117
da Cunha, E., Charlot, S., & Elbaz, D. 2008, MNRAS, 388, 1596
Davies, R. D., Elliott, K. H., & Meaburn, J. 1976, MNRAS, 81, 89
Dixon, W. V., Sahnow, D. J., Barrett, P. E., et al. 2007, PASP, 119, 527
Dufour, R. J. 1984, in IAU Symp. 108, Structure and Evolution of the Magellanic Clouds, ed. S. van den Bergh & K. S. de Boer (Dordrecht: Reidel), 353
Gordon, K. D., Bot, C., Muller, E., et al. 2009, ApJ, 690, 76
Gordon, K. D., Clayton, G. C., Misselt, K. A., Landolt, A. U., & Wolff, M. J. 2003, ApJ, 594, 279
Hilditch, R. W., Howarth, I. D., & Harries, T. J. 2005, MNRAS, 357, 304
Hutchings, J. B. 1982, ApJ, 255, 70
Kennicutt, R. C., Jr., & Hodge, P. W. 1986, ApJ, 306, 130
Kurucz, R. L. 1992, in IAU Symp. 149, The Stellar Populations of Galaxies, ed. B. Barbuy & A. Renzini (Dordrecht: Kluwer), 225
Malumuth, E. M., Waller, W. H., & Parker, J. Wm. 1996, AJ, 111, 1128
Maucherat-Joubert, M., Lequeux, J., & Rocca-Volmerange, B. 1980, A&A, 86, 299
Moos, H. W., Cash, W. C., Cowie, L. L., et al. 2000, ApJ, 538, 1
Murthy, J., Hall, D., Earl, M., Henry, R. C., & Holberg, J. B. 1999, ApJ, 522, 904
Murthy, J., & Sahnow, D. J. 2004, ApJ, 615, 315
Nandy, K., Morgan, D. H., & Carnochan, D. J. 1978, MNRAS, 184, 631
Pei, Y. C. 1992, ApJ, 395, 130
Pradhan, A. C., Pathak, A., & Murthy, J. 2010, ApJ, 718, L141
Sahnow, D. J., Moos, H. W., Ake, T. B., et al. 2000, ApJ, 538, 7
Vangioni-Flam, E., Lequeux, J., Maucherat-Joubert, M., & Rocca-Volmerange, B. 1980, A&A, 90, 73
Weingartner, J. C., & Draine, B. T. 2001, ApJ, 548, 296
Witt, A. N., & Gordon, K. D. 2000, ApJ, 528, 799